STAR: Science & Technology of Archaeological Research

ISSN: (Print) 2054-8923 (Online) Journal homepage: http://www.tandfonline.com/loi/ysta20

Variations in glutamine deamidation for a Châtelperronian bone assemblage as measured by peptide mass fingerprinting of collagen

Frido Welker, Marie A. Soressi, Morgan Roussel, Isolde van Riemsdijk, Jean-Jacques Hublin & Matthew J. Collins

To cite this article: Frido Welker, Marie A. Soressi, Morgan Roussel, Isolde van Riemsdijk, Jean-Jacques Hublin & Matthew J. Collins (2017) Variations in glutamine deamidation for a Châtelperronian bone assemblage as measured by peptide mass fingerprinting of collagen, STAR: Science & Technology of Archaeological Research, 3:1, 15-27, DOI: 10.1080/20548923.2016.1258825

To link to this article: http://dx.doi.org/10.1080/20548923.2016.1258825

Science and Technology of Archaeological Research

Research Article

Variations in glutamine deamidation for a Châtelperronian bone assemblage as measured by peptide mass fingerprinting of collagen

Frido Welker [1,2*], Marie A. Soressi [1,3], Morgan Roussel[3], Isolde van Riemsdijk [4], Jean-Jacques Hublin [1], and Matthew J. Collins [2]

[1]Department of Human Evolution, Max Planck Institute for Evolutionary Anthropology, 04103 Leipzig, Germany.
[2]BioArCh, University of York, York, YO10 5DD, United Kingdom.
[3]Faculty of Archaeology, Leiden University, Leiden, 2333 CC, The Netherlands.
[4]Biosystematics Group, Wageningen University, Wageningen, 6700 AA, The Netherlands.

Abstract Peptide mass fingerprinting of bone collagen (ZooMS) has previously been proposed as a method to calculate the extent of the non-enzymatic degradation of glutamine into glutamic acid (deamidation). Temporal and spatial variation of glutamine deamidation at a single site, however, has not been investigated. Here we apply ZooMS screening of Châtelperronian and Early Holocene bone specimens from Quinçay, France, to explore temporal and spatial variation in glutamine deamidation. Our results indicate that chronological resolution is low, while spatial variation is high. Nevertheless, our analysis allows the identification of bone specimens that have undergone diagenetic histories remarkably different (either in length or in type) from spatially related bone specimens. Therefore, ZooMS ammonium-bicarbonate screening is capable of testing bone assemblage homogeneity, which could guide subsequent analysis and interpretation.

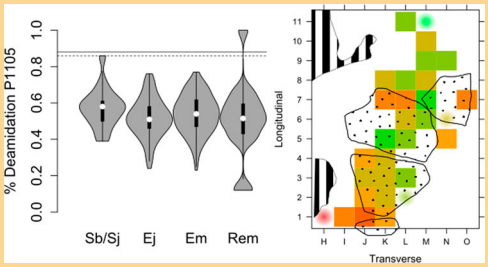

Keywords ZooMS; Châtelperronian; Diagenesis; Quinçay; Glutamine Deamidation; Bone

Subject classification codes Molecular biology

Received 30 May 2016; **accepted** 5 November 2016

Introduction

The presence of intrusive elements of younger or older age in archaeological bone assemblages is a key issue in Palaeolithic archaeology. Examples include a number of burials in Upper Palaeolithic contexts that were demonstrated to be Holocene in age by direct radiocarbon dating (Hoffmann et al., 2011; Conard et al., 2004; Terberger et al., 2001; Benazzi et al., 2014) or reworking of archaeological deposits by (micro)mammals (Enloe, 2012; Discamps et al., 2012). The unrecognized presence of intrusive elements could greatly influence the behavioral or ecological interpretation of a bone assemblage, and various approaches have therefore been proposed to assess the homogeneity of faunal assemblages (among others: Lyman, 1994; Behrensmeyer, 1978; Rendu et al., 2014; Blumenschine et al., 1996; Kuhn et al., 2010). These approaches either focus on preservation coherence, aim to identify the main accumulator(s), or study intrinsic bone properties such as surface modifications and bone density.

ZooMS (Zooarchaeology by Mass Spectrometry; Buckley et al., 2009) is used to establish the taxonomic composition of fragmented bone assemblages (Welker et al., 2015a; Brown et al., 2016; Evans et al., 2016; Charlton et al., 2016; Welker et al., 2016) and the taxonomic origin of worked artefacts (Fiddyment et al., 2015; von Holstein et al., 2014; Ives et al., 2014). A further potential application would be to assess faunal assemblage homogeneity as ZooMS is well suited for studying large numbers of bone and tooth specimens and requires small amounts of material

*Corresponding authors: F.W.: frido_welker@eva.mpg.de, and M.A.S.: m.a.soressi@leidenuniv.arch.nl.

DOI: 10.1080/20548923.2016.1258825

(commonly <30 mg). In this context, glutamine deamidation analysis has previously been suggested as a potential method of studying collagen preservation variability and for the detection of potential outliers (van Doorn et al., 2012; Simpson et al., 2016; Schroeter & Cleland, 2016). Glutamine deamidation ratios can be obtained during routine ZooMS screening of faunal samples when adequate extraction protocols are followed (van Doorn et al., 2012; van Doorn et al., 2011). Up to now, however, spatial or chronological variability of glutamine deamidation at a single site has not been studied. Therefore, in this study we perform ammonium-bicarbonate ZooMS screening (van Doorn et al., 2011) on a total of 543 bone and dental specimens from Quinçay, France to address this lack of data.

The site of Quinçay is ideal for exploring deamidation variation as it contains an archaeological sequence with scattered Holocene bone specimens lying on top of several *in situ* Châtelperronian units, likely older than 40ka cal BP, with no indication of elements of intermediate chronological age (Lévêque et al., 1997; Roussel & Soressi, 2010; Roussel, 2013; Roussel et al., 2016). Some of the bone specimens found at the surface might even be very recent. Furthermore, the Châtelperronian units at Quinçay contain six pierced animal teeth that are interpreted as beads or personal ornaments (Granger & Lévêque, 1997). Objects such as these, thought to have had "symbolic" meaning, play a pivotal role in discussions on late Neanderthal behavior and the biological attribution of the Châtelperronian (Caron et al., 2011; Higham et al., 2010; Hublin et al., 2012; Soressi & Roussel, 2014; Welker et al., 2016). In this study, we describe variations in glutamine deamidation between archaeological units as well as spatial variation within archaeological units. Next, we discuss the possible interpretational value of these results in relation to specific sedimentary features or artefacts present at the site.

Material and methods

Quinçay

Excavated between 1968 and 1990 by François Lévêque, the Grande Roche de La Plématrie at Quinçay (France) is a limestone cave facing the south/south-east in a dry tributary to the river Auxance (Lévêque & Miskovsky, 1983). The small cave is broadly divided into a front area, where limestone blocks (numbered with Roman numerals I to V) cover part of the stratigraphy, and a back area, where such limestone blocks are absent (Roussel et al., 2016). The naming of sedimentary/archaeological units generally follows this division between the front area (units named 'Ensemble', or starting with 'E') and the back area (units named 'Série', or starting with 'S'). During the excavation, lithics and faunal specimens were collected and recorded by stratigraphic units, with subunits usually 5 or 10 cm thick.

The youngest material was found at the back of the cave on top of the stratigraphic sequence, where Lévêque et al. (1997) collected seven Mesolithic lithics on the surface. An additional 10 ceramic fragments attributed to the early Neolithic were found on the surface in the same area. The lithics found in the frontal part of the cave have been described by Lévêque (1979) and have recently been studied by M. Roussel (Roussel et al., 2016). The units Ej, Em and En have been attributed to the Châtelperronian, while the bottom unit Eg has recently been reattributed to the Mousterian of Acheulian Tradition Type B (Roussel & Soressi, 2010). According to unpublished stratigraphic documentation by F. Lévêque, a correlation can be established between the units from the front part of the cave and the units found in the back of the cave (Table 1). The chronological position of units So and Sb is less clear. In addition, a small quantity of finds was discovered in reworked sediments present in square 4L. These specimens have been assigned by F. Lévêque to a unit called 'remanié' (French: 'reworked'), with excavation notes describing the extent of this feature within the square. From these notes, however, the age of the disturbance or of the material contained within it is unknown.

Faunal remains are preserved mostly within the upper layers (Ej+Sj and Em+Sm), and a paleontological analysis of identified specimens has been published (Lavaud-Girard, 1986). Five out of six pierced teeth come from the front area of the cave, while the sixth originates from the back area. They were all found in the upper layers of the site; five come from layer Em and one from the bottom of layer Ej. They have previously been described (Granger & Lévêque, 1997).

In this study, we measure glutamine deamidation for a large sample of previously unidentified faunal specimens. We compare the glutamine deamidation values from the front area (Ensemble) with the values obtained in the back area (Série) for the various units for which material was studied, including the 'remanié', in both temporal and spatial frameworks. From the notebooks and unpublished documents, the expectation is that all the faunal remains should be of Châtelperronian age, except maybe some specimens found within the units So, Sb and the 'remanié'. We will also briefly discuss the homogeneity of the deamidation values obtained on faunal specimens excavated in close proximity to the pierced teeth.

ZooMS COL1 extraction

Faunal samples were taken from 475 morphologically undiagnostic cortical bone specimens (246 for units Ej+Sj, 222 for units Em+Sm, 28 for units En+Sfi) by random selection. Although Lavaud-Girard (1986) mentions the presence of three identified bone

Table 1 Stratigraphic correlation between the front and the back areas at Quinçay, and their cultural attribution (when known). Subunits are indicated between brackets.

Ensemble	Cultural attribution Ensemble	Série
		Sb
		So
Ej (o, m, p, j)	Châtelperronian	Sj
Em (o)	Châtelperronian	Sm
Emf	Châtelperronian	Sfs
Emj	Châtelperronian	Sfj
En (m, n, c)	Châtelperronian	Sfi
Eg (j, f, c, b)	MTA-B	Sg

specimens from unit Eg, no bone specimens of this unit were included in the present study. Additionally, we identified and sampled bone and dental specimens from above unit Ej+Sj (n=18 for samples assigned to a combined Sb/Sj and n=3 for unit Sb). Sample sizes for these two units are small due to their limited spatial extent. Further, we sampled 26 specimens from the 'remanié' located in square 4L, to test whether unusual deamidation values were present in this feature compared to surrounding squares. Combined, the total number of studied specimens is 543.

Collagen (type I, COL1) was extracted following the protocol outlined by van Doorn et al. (2011). This protocol not only allows calculation of deamidation values without inducing deamidation during protein extraction, but it also facilitates subsequent study of the sample itself by further analyses that would require demineralization. This protocol thereby reduces the need to re-sample the original bone specimen. Such subsequent analyses could include additional ZooMS verification using bone demineralization (Welker et al., 2015a), proteomic LC-MS/MS analysis (Welker et al., 2015b) or ancient DNA analysis (von Holstein et al., 2014).

Bone samples weighing between 10–30 mg were immersed in 100 µl ammonium-bicarbonate buffer (50 mM) for one day at room temperature. Next, the samples were centrifuged, the buffer removed and the sample re-immersed in 100 µl ammonium-bicarbonate (50 mM) for 1 hour at 65°C. Afterwards, 50 µl of ammonium-bicarbonate buffer, now containing eluted soluble collagen, was transferred to a new Eppendorf. Protein digestion was accomplished by adding 1 µl of trypsin (Promega) and incubation at 37°C overnight. 1 µl of TFA (5%) was added to quench the enzymatic digestion, and peptides were purified on a C_{18} ZipTip (Agilent) with elution in 50 µl of 50% can in 0.5% TFA (Welker et al., 2015a). Species identification was based on peptide markers for relevant species published previously (Buckley et al., 2009; Welker et al., 2016). In case ammonium-bicarbonate buffer extraction failed to provide useful taxonomic information, the same bone sample was demineralized in acid and processed again (following Welker et al., 2015a; Welker et al., 2016). A method blank containing used reagents was processed alongside archaeological samples to check for the presence of COL1 contamination during ZooMS screening, the results of which were negative.

Glutamine deamidation calculation

Glutamine (Q) deamidation was calculated for ammonium-bicarbonate ZooMS spectra for two of the peptides studied by van Doorn et al. (2012; Wilson et al., 2012)). The studied peptides, P1105 (GVQGPPGPAGPR, *COL1α1*) and P1706 (DGEA-GAQGPPGPAGPAGER, *COL1α1*), have an identical amino acid sequence in the terrestrial species studied here, thereby removing a potential confounding influence of the primary amino acid sequence on observed deamidation rates (Robinson & Robinson, 2001). They contain only a single possibly deamidating position, and have low deamidation rates compared to other glutamine positions in COL1 (van Doorn et al., 2012), ensuring that saturation is not reached in Late Pleistocene contexts. We report deamidation ratios to range from %Gln=1.0, non-deamidated glutamines, to %Gln=0.0, fully deamidated glutamines. This change can be observed as a shift in the isotope distribution of the peptides (Figure 1). Deamidation ratios were calculated with a signal-to-noise ratio of 4.0, Fitpeaks at 3.0, Fitnoise at 2.0 and with mass steps equal to 0.1 m/z.

Statistical analysis

To distinguish outliers or possible sub-groups among the %Gln values we 1) constructed boxplots with whiskers ranging 1.5 times the interquartile range (IQR), 2) performed a Grubbs test, and 3) calculated density curves. Any %Gln value over 1.5 IQR will be identified by the boxplots as a non-parametric outlier. We tested each of these by performing Grubbs test, designed to parametrically identify outliers when dealing with small sample sizes. We employ 3 versions of Grubbs test, designated to identify **a)** one outlier on one tail, **b)** two outliers, each on one tail, and **c)** two outliers on one tail. Grubbs test identifies significant outliers when $p \leq 0.05$. Density curves are constructed with a kernel width of h=0.04. Density curves and boxplots are presented as violin plots, where the boxplot is centrally integrated within the density curves.

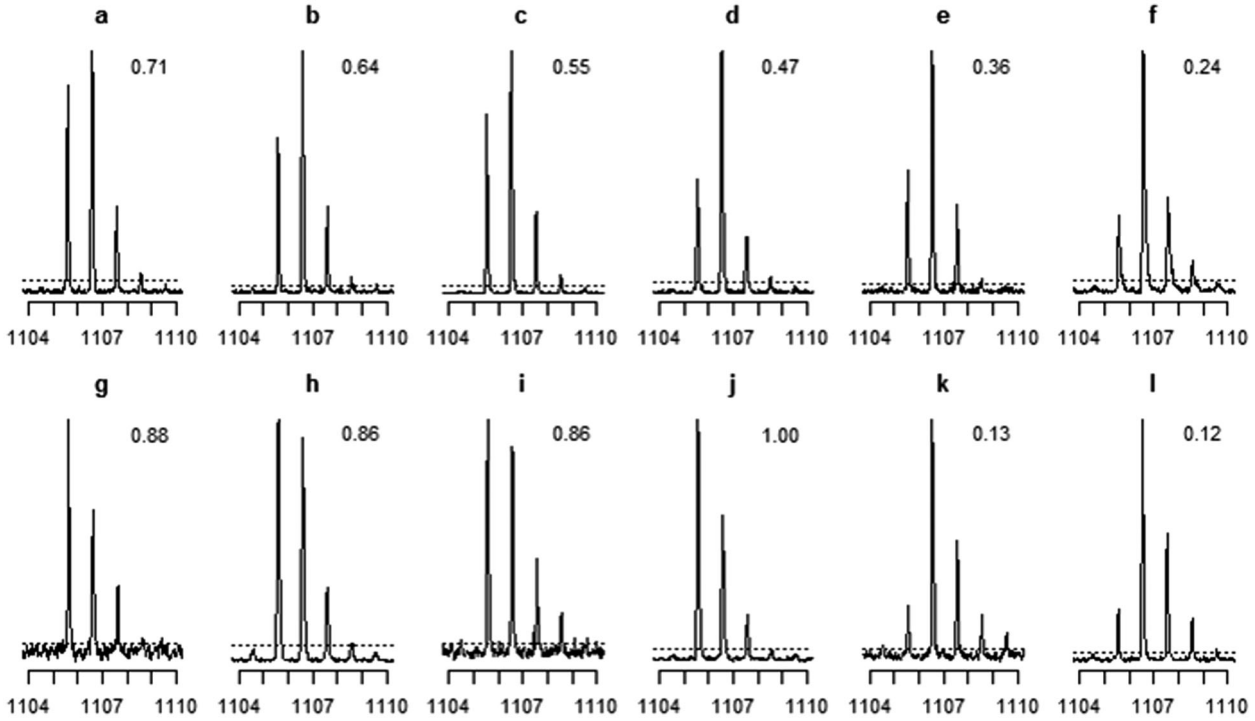

Figure 1 Example spectra showing variation in glutamine deamidation for P1105 (GVQGPPGPAGPR). a-f) General examples from %Gln 0.71 to 0.24. g) Value obtained for unit Sb. h) Value obtained for unit Sm. i) Value obtained for unit Sb/Sj. j-l) Values obtained for the 'remanié'. All spectra range between 1104 and 1107 m/z with intensity scaled relative to the most intense peak in this mass window. Dotted lines indicate approximate local signal-to-noise ratio of 4.0.

Table 2 Faunal identifications in NISP by ZooMS per archaeological unit. Following Lavaud-Girard 1986, Equidae includes horse (*Equus caballus*) and European ass (*Equus hydruntinus*), Rhinocerotidae concerns Woolly rhino (*Coelodonta antiquitatis*) Cervid/Saiga includes red deer (*Cervus elaphus*) and Elephantidae concerns Woolly mammoth (*Mammuthus primigenius*).

	Sb	Sb/Sj	Ej	Sj	Em	Sm	En	Sfi	Rem
Bos/Bison		1	36	9	34	2	5		5
Bos/Bison/Muskox			2	1	3		3		
Equidae	1	4	60	22	72	10	10		5
Rangifer		8	34	37	51	17	2		3
Cervid/Saiga			1		3				
Sheep/Chamois			1		2				
Suidae			4						
Elephantidae				1	2	2	4	4	
Rhinocerotidae			3		2	1			
Leporidae	2		3	1	2				3
Ursidae		5	1		1				
Hyaenidae			1		2				
Canidae (not red fox)			4	1	3	1			
Red fox			1						1
Felinae				1					
Taxonomic group:									
Bovidae				1		1			
Bovidae/Cervidae			2		2	1			
Bovidae/Cervidae/Equidae			6	4	3	2			
Bovidae/Rangifer			2	2					
Caprinae/Rangifer			1			1			
Caprinae/Saiga/Cervidae				1					
Felidae/Ursidae			1						
Hyaenidae/Pantherinae									1
Indeterminate			1	1	1				8
Total	**3**	**18**	**164**	**82**	**183**	**39**	**24**	**4**	**26**

Results

ZooMS species identification and species composition

Out of 543 bone and tooth specimens, 11 specimens (2.0%) could not be identified, 31 specimens (5.7%) were attributed to taxonomic groups that could be specified further if missing peptide markers had been present and 501 bone specimens (92.3%) could be identified to family, genus or species level (Table 2). We note that 8 out of 11 unidentified specimens are located in the 'remanié'. To achieve this success rate, 29 bone specimens needed to be demineralized after ammonium-bicarbonate buffer extraction (5.3% of the studied assemblage).

Comparison with two previous studies of the Quinçay fauna assemblage (Lavaud-Girard 1980, 1986) reveals a rather similar species composition between those studies and this study. We note the addition of *Sus* sp. (Suidae) to unit Ej by ZooMS screening. This taxon was also added by ZooMS to the Châtelperronian at Les Cottés (Welker et al., 2015a). Mustelidae are absent in the ZooMS assemblages studied, while Lavaud-Girard (1986) mentions the presence of weasel (*Mustela* sp.) and Marten (*Martes martes*) in units Ej and Em. This could potentially be explained by the absence of sampling complete, identifiable teeth for the ZooMS samples studied here.

Glutamine deamidation

Glutamine deamidation ratios for peptide P1105 could be calculated for 457 spectra from ammonium-bicarbonate extracts, of which 16 are dental specimens (see Figure 1 for examples). P1706 was observed in a smaller number of instances (n=266 in total, n=12 dental specimens). We excluded P1706 on the basis of a smaller number of observations for the spatial analysis presented here, and we also excluded dental specimens (unless specified otherwise). Glutamine deamidation values for all included bone specimens are attached in Supplementary Table 1.

Glutamine deamidation ratios are not correlated with bone length (Pearson R=0.051; Figure 2B) or species identification when divided into small, medium, large and megafauna size classes (ANOVA, F(3)=0.374, p=0.77). As we mostly sampled cortical bone specimens, intrinsic bone specimen properties such as bone length, taxonomic origin or bone type therefore do not explain any variation observed in deamidation.

In plan view, values for units Ej, Sj, Em and Sm indicate a relatively heterogeneous %Gln distribution within the cave (Figure 2A). Despite the overall heterogeneous composition, several patterns are apparent when looking at transverse and longitudinal cross-sections of the cave (Figure 3). Transverse deamidation values are lowest in the "I" squares, for both units

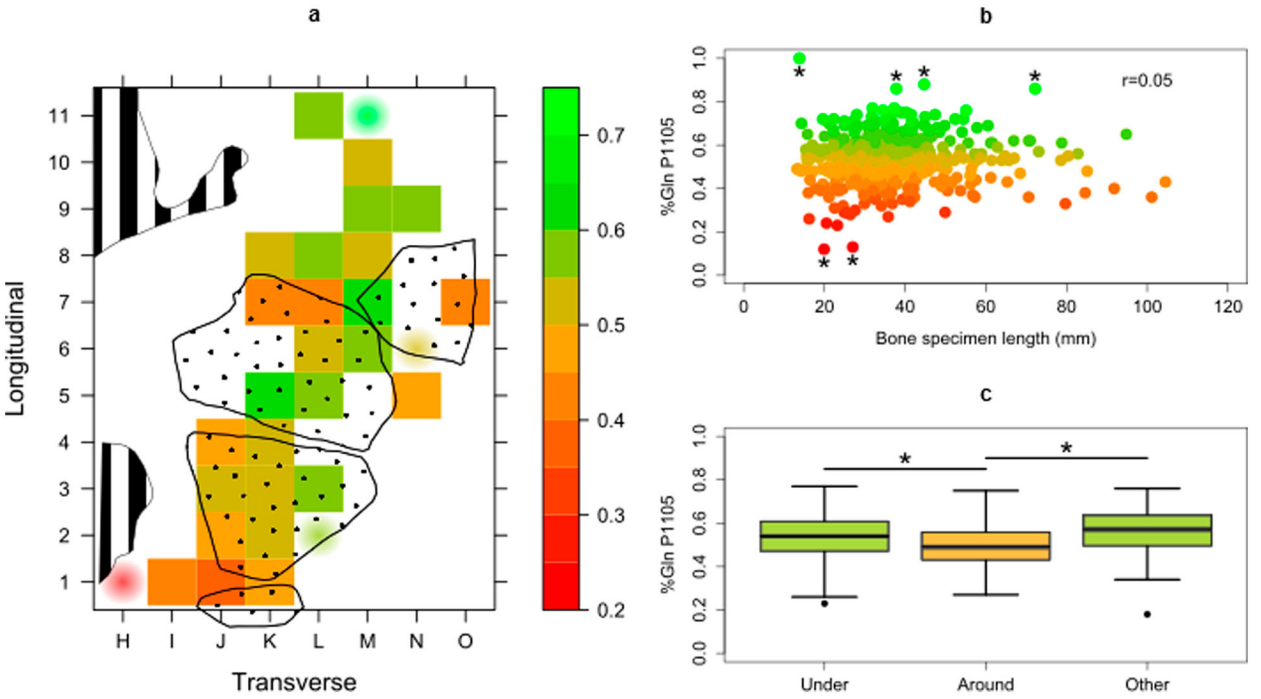

Figure 2 Variation in P1105 glutamine deamidation ratios. (a) Mean %Gln for P1105 by square for units Ej, Em, Sj and Sm. The approximate position of several limestone blocks on top of the main sequence is superimposed and filled with dots. Cave wall limits are delimited by the hatched lines on the left hand side. Squares with a single measurement are indicated by transparent circles. (b) A correlation between bone specimen length (in mm) and P1105%Gln deamidation is absent. Samples with significantly deviating values, following Figure 4, are indicated with asterisks (*). (c) Boxplots of P1105 deamidation ratios observed for squares located under the limestone blocks, those directly around these blocks and squares located further away (rows 9–11). Statistically significant differences are indicated (p<0.05, *).

(Figure 3B). Although based on a small number of measurements, these squares are closest to the limestone wall of the cave. It is well known that water movement in caves has a significant influence on bone preservation, for example by precipitation along cave walls causing increased mineral dissolution in peripheral cave areas (Bocherens et al., 2008; Salesse et al., 2014). We hypothesize that such processes are indicated by our deamidation data in transverse view for square 1I and 1H.

The longitudinal cross-section (Figure 3A) reveals very similar patterns for units Ej+Sj and Em+Sm. Deamidation values are lowest in squares along row 1, and are constant throughout most of the other rows except for row 7 where there is a dip towards lower values. Low values at the front of the cave (squares 1I, 1J and 1K) can (also) be explained by increased hydrological activity along the rock face containing the cave (eg. an active dripline). The sudden dip in row 7 corresponds with the end of limestone block III. We find significant differences between squares located under the limestone blocks (%Gln P1105 =0.54±0.11) compared to squares directly around the edges of these limestone blocks (0.49±0.11; t (124.01)=3.16, p=0.00). We find no significant differences between squares under the blocks and those located further away from the edges of these blocks in rows 9–11 (0.56±0.11; t(106.07)=-1.60, p=0.11), but do find significant differences between squares along the edges of the blocks and those further away (t (136.27)=−3.79, p=0.00). This suggests that the squares around the blocks are deamidated more than other squares, possibly because the limestone blocks cause water precipitation to run off alongside the edges of these blocks (Figure 2C). A relatively similar scenario has been proposed to explain areas with differing bone preservation at Hayonim Cave (Stiner et al., 2001). From these observations and comparisons it is clear that deamidation values of individual bone specimens reflect both localized conditions (the presence/absence of limestone blocks) and processes common to caves in general (the presence of a dripline, positioning relative to wet cave walls).

No significant differences in deamidation ratios could be observed between the Châtelperronian units (Ej, Sj, Em, Sm, En and Sfi; Figure 4), although the spread in %Gln values is large. Violin plots and the boxplots included within them indicate the presence of non-parametric outliers at the positive end (towards 1.0) for units Sb/Sj (Figure 1I), Sm (Figure 1H) and within the 'remanié' (Figure 1J), and at the negative end (towards 0.0) for the 'remanié' (Figure 1K-L). These will be discussed individually below. The same bone specimens and their associated %Gln P1105 values are also identified as outliers when the data are considered by square, in addition to several outliers in square 9N. These outlying values from square 9N are within the %Gln distribution observed elsewhere, but they are identified as outliers by Grubbs test (Table 3). For square 3J, one specimen had a negative outlying value compared to other values for this square, but was not identified by the Grubbs test as an outlier (Table 3). We do not consider these further.

Deamidation values for a single 'remanié'.

A total of 26 bone specimens from square 4L were studied coming from a 'remanié', a sedimentary unit composed of reworked material. Bone specimens designated as coming from this feature span a depth of 40 centimetres, encompassing the full depth of this feature as described in the excavation notebooks. The majority (8/11) of the unidentified specimens come from this feature. Analysis of glutamine deamidation values from the remaining bone specimens indicate both non-deamidated (1.0; Leporidae specimen, Figure 1J) and highly deamidated specimens (0.12/0.13; Bos/Bison specimens, Figure 1K-L). The majority of bone specimens have deamidation values similar to those obtained for surrounding squares for units Ej and Em (Figure 1A-F, Figure 5). Both the

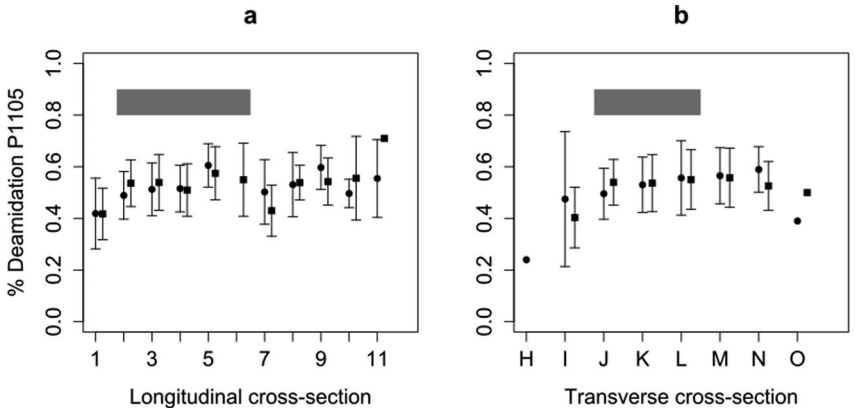

Figure 3 Glutamine deamidation ratios for peptide P1105 in longitudinal cross-section (a, squares 1>11) and transverse cross-section (b, squares H>O) of the cave. The limestone blocks on top of the main sequence from squares J2 to M6 are indicated by the gray bar. Error bars are 1SD around the mean calculated for each archaeological unit. Ej+Sj: circles, Em+Sm: squares.

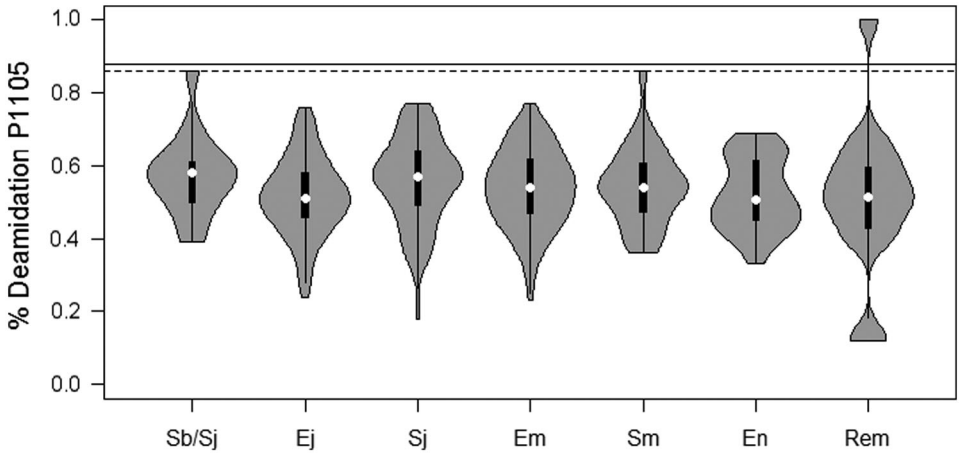

Figure 4 Violin plots for bone P1105 glutamine deamidation ratios of individual units and the 'remanié' (Rem). Width of violins depicts a kernel density probability for all included values per archaeological unit. Boxplots at the center correspond to the median (open circle), 25 and 75% quantiles (black bars) and 1.5 interquartile ranges (whiskers). The single value for unit Sb (0.88) is indicated by the upper solid line. The lower dashed line corresponds to two values present in the combined unit Sb/Sj and unit Sm that are comparable (0.86). %Gln measurements for unit Sfi are excluded due to small sample size for this unit. Violins reach to the minimum/maximum value present without further smoothing.

Table 3 Statistical outlier tests for squares 3J, 4L, 9N, 10K and 10M. Fractions include all measurements ('Total'), those composed of the boxplot and positive outliers ('Upper'), or those composed of the boxplot and negative outliers ('Lower'). Grubbs test for 2 outliers on one tail requires sample size to be between 3 and 30 and was therefore not calculated for square 3J. All archaeological units are included.

Square	Fraction	Boxplot outlier (Yes/No)	Grubbs test A (*p*)	Grubbs test B (*p*)	Grubbs test C (*p*)
3J	Total	Yes	0.11	0.35	
4L ('*remanié*')	Upper	Yes	0.00	0.11	0.01
4L ('*remanié*')	Lower	Yes	0.14	1.00	0.00
9N	Upper	Yes	0.08	1.00	0.02
9N	Lower	Yes	0.14	0.38	0.03
10K	Total	Yes	0.04	0.10	0.08
10M	Total	Yes	0.02	0.11	0.04

boxplot and the Grubbs test indicate that the high and the low %Gln values are statistical outliers (Table 3). Therefore, this reworked feature contains some material that has undergone diagenetic processes different (either in nature or in length) from those of neighbouring squares, with the majority of bone specimen %Gln values comparable to neighbouring squares. The outlying values were observed for bone specimens that were excavated at the bottom of the 'remanié' (Figure 5).

Deamidation values for units Sb and Sb/Sj.

At the back of the cave the presence of additional sedimentary units above unit Sj has been noted (Table 1). On top of unit Sb, isolated lithic and ceramic artifacts are present, attributed to Holocene time periods (Lévêque et al., 1997). In addition, detailed drawings of the cave surface indicates the presence of a concentration of artefacts on the surface, as well as a possible shallow pit in the area of squares 11M/11N/12M/12N (Roussel et al., 2016). The extent of this feature is not known.

Three bone specimens from unit Sb were sampled. To these can be added 18 bone specimens associated with a sedimentary unit that potentially includes material from both Sb and Sj (termed unit Sb/Sj). We find that the one %Gln value we obtained for unit Sb is significantly less deamidated compared to the values obtained for units Ej+Sj, Em+Sm and En+Sfi (%Gln=0.88, Figure 4, Figure 1G). This bone specimen originates from square 11K, for which no additional specimens were available.

Importantly, we identify a comparable value in unit Sb/Sj (square 10K, %Gln P1105 = 0.86, Figure 1I), suggesting that material attributed to this sedimentary unit indeed comprises a mixture of material. This value is identified as an outlier compared to other %Gln values obtained for this square by both the non-parametric boxplot and the parametric Grubbs test (Figure 6; Table 3). These values are approximated by one additional bone specimen in square 10M (%Gln P1105 = 0.86, Figure 1H), which is attributed to unit Sm. Again, this specimen is an outlier in our analysis by square, as well as an outlier for the unit Sm (Figures 4 and 6; Table 3). This specimen potentially

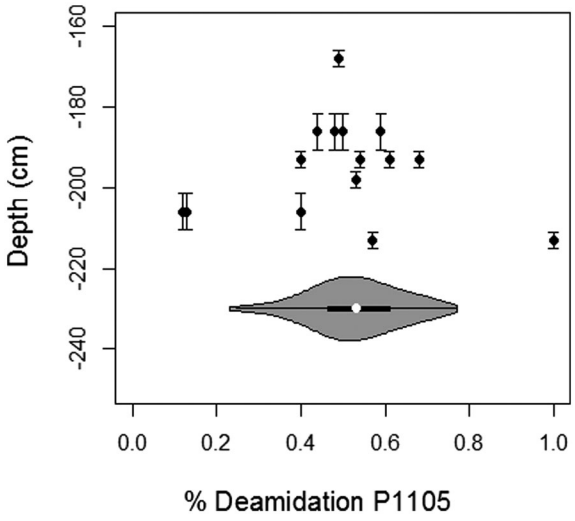

Figure 5 Deamidation values by depth below datum for the 'remanié' in square 4L. Error bars indicate minimum and maximum depth below datum of the spit in which the bone specimens were excavated. Violin plot at the bottom indicates glutamine deamidation distribution for units Ej and Em as a comparison.

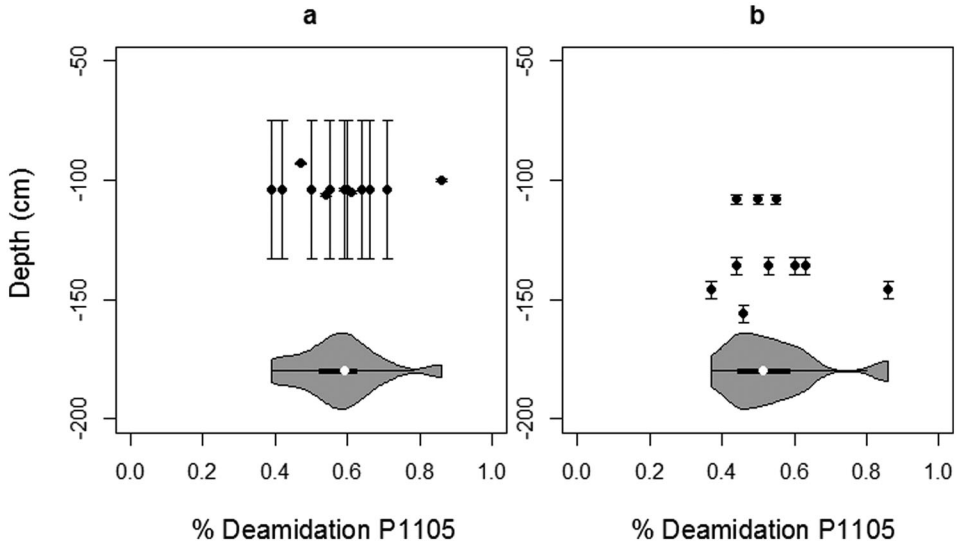

Figure 6 Deamidation values by depth below datum for squares 10K (a) and 10M (b). Error bars indicate minimum and maximum depth of the spit in which the bone specimens were excavated.

represents intrusive material unrecognized during the excavation of this square, or might represent an exceptionally well-preserved bone specimen (Schroeter and Cleland 2016). Direct radiocarbon dating of this bone specimen could confirm or refute either hypothesis, as we realize that the number of bone specimens securely attributed to unit Sb is unfortunately small.

Discussion

Glutamine deamidation and spatial variation.

So far, three published studies have reported on glutamine deamidation ratios in archaeological bone collagen measured by MALDI-TOF-MS (van Doorn et al., 2012; Simpson et al., 2016; Welker et al., 2016) while several other studies report on ancient bone protein deamidation investigated through LC-MS/MS analysis. Mikšík et al. (2014) discuss the deamidation of glutamines and asparagines in a Medieval mummy from Verona, Italy. Based on LC-MS/MS measurements, the deamidation was noted as present or absent for individual glutamine or asparagine positions. Overall, 77.9% of the assigned glutamines were deamidated in bone (Mikšík et al., 2014). For both peptides studied here, their study notes the presence of a deamidated glutamine, not unexpected given the environmental conditions at which the mummy was deposited (Mikšík et al., 2014). Also based on LC-MS/MS data, two other studies presented collagen deamidation data for various Pleistocene mammals (Welker et al. 2015b; Orlando et al., 2013). Undated mammoth and horse

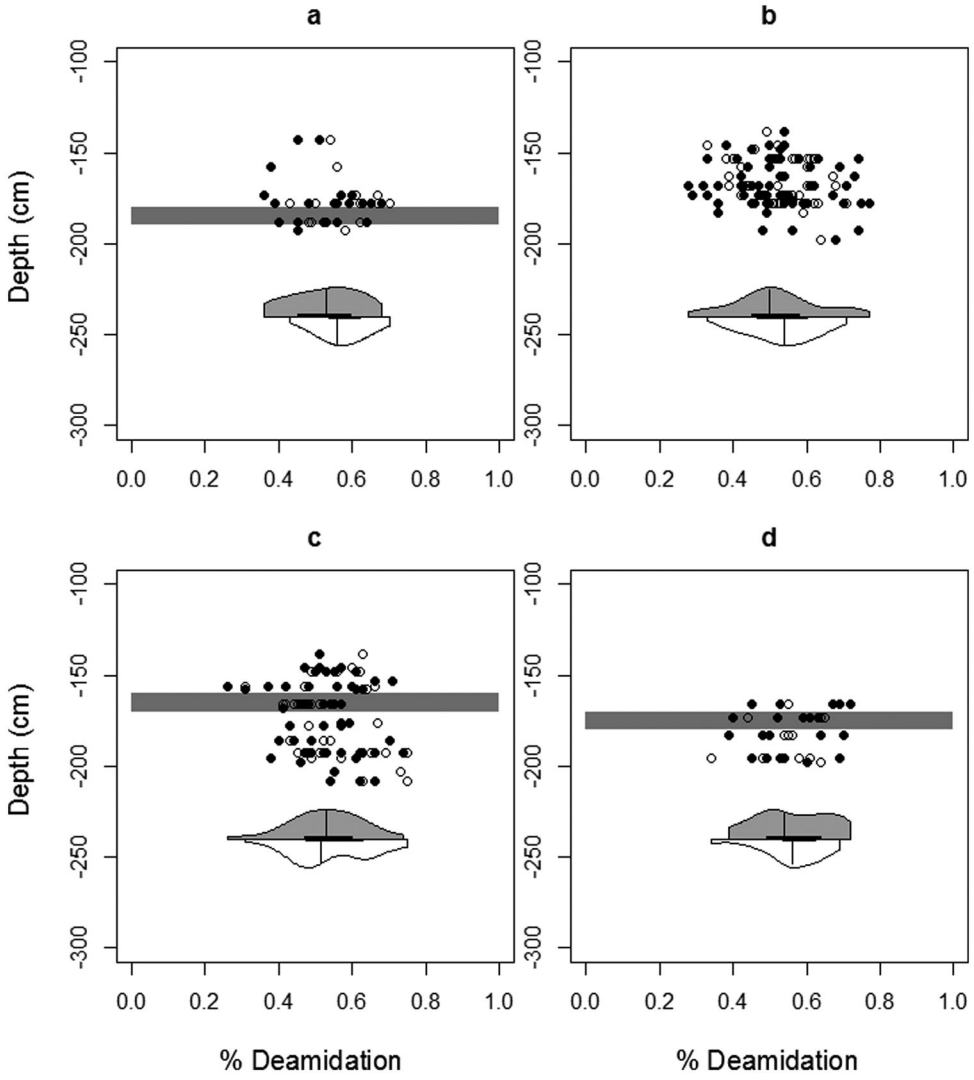

Figure 7 Deamidation context for the pierced teeth found in squares (a) 2K, (b) 3K, (c) 3J, and (d) 5L. Only bone specimens with a spit accuracy of 10 cm or less are included. Note that squares 2K, 3J and 5L are covered by the limestone blocks. Filled symbols: P1105. Open symbols: P1706. Violin plots per peptide are included at the bottom, with shading similar to the points. Shaded regions indicate the approximate depth at which the Quinçay beads were found, which is unknown for the two beads in square 3K.

bones presented average glutamine deamidation in 45.9% and 42.9% of observations for permafrost samples and 82.2% and 76.1% for temperate samples (Orlando et al., 2013). The deamidation frequency for individual glutamine positions is not reported in this study, however, and so comparison of specific amino acid positions with other studies is difficult. In a context chronologically younger than that of the Middle Pleistocene horse, deamidation ratios were obtained for directly dated *Toxodon* specimens (59.2±24.5% for P1105), *Macrauchenia* bone specimens beyond the radiocarbon limit (82.8 ±14.3% for P1105), and an undated but presumably younger horse specimen (18.9±18.4%; all data from (Welker et al., 2015b). For these specimens, the variation between deamidation ratios of a single bone specimen and those between different bone specimens might be a reflection of environmental conditions rather than chronological factors, despite that the age of some of these bone specimens is unknown (Schroeter & Cleland, 2016).

It has been demonstrated elsewhere that some protein extraction procedures can induce deamidation during demineralisation and/or once proteins becomes solubilized (Ren et al., 2009; Hao et al., 2011; Simpson et al., 2016), and these extraction procedures generally differ between published sources. All of the aforementioned studies, except for van Doorn et al. (2012), Welker et al. (2016) and some of the data presented in Simpson et al. (2016), employed slightly different extraction conditions and so direct comparisons between datasets are difficult. The extraction procedure used here, in van Doorn et al. (2012), Welker et al. (2016) and in some data reported in Simpson et al. (2016), is identical and optimized to extract already soluble protein from the bone microenvironment (van Doorn et al., 2011; 2012). Previously, it has been demonstrated that this extraction protocol does not induce

deamidation for the studied peptides when performed on modern bone samples (Welker et al., 2016). Furthermore, we focused our main analysis on one collagen peptide (P1105) that has an identical primary amino acid sequence between the different terrestrial species included in the study, thereby removing a potential confounding effect of the primary amino acid sequence on glutamine deamidation rates (Robinson & Robinson, 2001; Robinson et al., 2004).

The variation in %Gln observed for P1105 in several sites from the van Doorn et al. (2012) study and for the Châtelperronian units at Quinçay is large. This variation might be a reflection of localized geological and environmental conditions, rather than chronology, and is in agreement with suggestions made elsewhere (Schroeter & Cleland, 2016). Such variation has not been investigated more specifically previously but could explain part of the %Gln variation of any given site. For Les Cottés, previous deamidation data for peptide P1105 is similar to those obtained here for Quinçay (van Doorn et al., 2012) and at the Grotte du Renne (Welker et al., 2016). At Les Cottés, the stratigraphy includes sterile layers separating some archaeological horizons, including sterile units around the studied Châtelperronian stratigraphic unit 06 (Talamo et al., 2012). Therefore, the sterile sediments are an argument against the observed variation in %Gln being the result of younger intrusions.

Our workflow enables large-scale explorations of %Gln variation at a site, both spatially and temporally, when a sufficient number of samples are included. From a taphonomy point of view, any outlying bone specimens could subsequently be selected for more expensive and destructive analysis such as radiocarbon dating. This would enable a more directed radiocarbon dating program to be undertaken in order to understand the chronological composition of a bone assemblage, as it has recently been demonstrated that successful ZooMS analysis often also results in successful collagen extraction for AMS radiocarbon dating of the same bone specimen (Harvey et al., 2016). A comparative radiocarbon chronology for Quinçay is currently lacking, and, unfortunately, several of the bone specimens identified as statistical outliers here are too small for direct AMS radiocarbon dating.

From a spatial point of view, ZooMS ammonium-bicarbonate screening could be employed as a powerful method of screening bone preservation between excavation seasons, thereby directing subsequent excavation and bone specimen sampling decisions. For example, ZooMS has previously been combined with other biomolecular analyses such as dietary stable isotope analysis (Vaiglova et al., 2014; Charlton et al., 2016), ancient DNA analysis (Evans et al., 2016; von Holstein et al., 2014; Meiri et al., 2014), or additional palaeoproteomic analysis using LC-MS/MS (Welker et al., 2015b; Welker et al., 2016). The heterogeneity in %Gln values among the 'bulk' %Gln values present in a given square or sedimentary unit might be used to inform bone specimen selection for additional biomolecular analysis (aDNA, palaeoproteomics) towards those specimens with less deamidation. In this regard, future work should focus on exploring a possible correlation between collagen deamidation, DNA deamination and biomolecule fragmentation (for example DNA sequence length or non-enzymatic protein cleavage frequency), as both deamidation and deamination are temperature dependent and pH dependent (Lyndahl & Nyberg, 1974; Scotchler & Robinson, 1974; Catak et al., 2009; Allentoft et al., 2012).

The deamidation context of the Quinçay pierced teeth.

The Quinçay pierced teeth are, together with the Châtelperronian personal ornaments at the Grotte du Renne, Arcy-sur-Cure, unique cultural artefacts attributed to Châtelperronian Neanderthals (Hublin et al., 1996; Granger & Lévêque, 1997; Caron et al., 2011; Welker et al., 2016). The stratigraphic placement of these items is, therefore, of importance in understanding and interpreting late Neanderthal behavior (Roussel et al., 2016). We present glutamine deamidation data spatially related to these items, but could not study the ornaments themselves.

All pierced teeth come from the lower part of unit Ej (square 3J) or the upper part of unit Em (squares 2K, 3K, 5L and 10L). No comparative faunal material has been studied from square 10L, despite attempts to locate such specimens. For the tooth found in this square and for one of the two found in square 3K no

Table 4 Deamidation data related to the Quinçay pierced teeth. Grubbs test for 2 outliers on one tail requires sample size to be between 3 and 30 and was therefore not calculated for squares 3J and 3K.

Bead	Unit	Square	Morphological identification	%Gln P1105	%Gln P1706	Grubbs test A (*p*)	Grubbs test B (*p*)	Grubbs test C (*p*)
1 + 2	Em	3K	*Vulpes vulpes*	0.52 ± 0.11	0.53 ± 0.09	0.88	1.00	
3	Em	10L	*Vulpes vulpes*					
4	Ejm-base	3J	*Canis lupus*	0.53 ± 0.10	0.54 ± 0.11	0.11	0.35	
5	Emf	5L	*Cervus elaphus*	0.56 ± 0.10	0.56 ± 0.09	0.83	1.00	0.56
6	Em	2K	*Cervus elaphus*	0.52 ± 0.09	0.57 ± 0.07	0.83	1.00	0.63

precise stratigraphic provenance is available, although both are assigned to unit Em.

We tested non-parametrically for the presence of outliers using boxplots (Figure 7), but found no outliers in the tested squares for P1105 above 1.5 IQR. Testing for the presence of one or two outliers, the Grubbs test further indicates the absence of a statistical outlier in the relevant squares (Table 4). Neither do we observe the presence of a relationship between burial depth and deamidation values (Figure 7) or aberrantly high or low %Gln values at the approximate depth the pierced teeth were found.

Taken together, for each square the %Gln for P1105 and P1706 indicate that the sampled bones constitute a single population without values similar to that of modern bone specimens or those obtained for unit Sb. The wide spread in deamidation data obtained here, and elsewhere, precludes any significant statements on the presence of intrusions chronologically close in time to the Châtelperronian units. Based on archaeological observations the Quinçay pierced teeth are of a Châtelperronian origin.

Conclusion

Assessing and understanding bone assemblage homogeneity/heterogeneity is often central to subsequent analysis, such as faunal analysis, palaeoproteomics or aDNA. Here we demonstrate that ZooMS ammonium-bicarbonate screening is capable of highlighting particular patterns in glutamine deamidation, both in spatial and temporal contexts. As demonstrated before, chronological resolution is low or absent. Therefore, our analysis allows identifying bone specimens that have undergone different diagenetic histories (either in length or type). As such elements could represent intrusive material, ZooMS allows such specimens to be selected from a larger sample set for subsequent analysis. In this regard, the identification of bone specimens with glutamine deamidation ratios similar to modern bone specimens in a reworked feature ('remanié') at Quinçay highlights the potential of such ZooMS screening. In addition, future comparisons between glutamine deamidation, DNA deamination and biomolecular fragmentation of DNA and proteins could potentially be used to identify bone specimens that are more suitable for subsequent biomolecular analysis through ZooMS analysis. The results are promising as the analysis is applicable to bone assemblages studied using ZooMS without additional costs.

Acknowledgements

We thank Freek Bakker (Wageningen University) for his supervision of I.v.R. during her MSc at Wageningen University (the Netherlands). S. McPherron is thanked for comments on a previous version of this paper. Keri Rowsell, Luke Spindler and Annabell Reiner are thanked for technical support. This research was made possible by funding through the Max Planck Institute for Evolutionary Anthropology (Leipzig, Germany).

Author biographie

F.W. is a PhD student at the MPI-EVA, Leipzig, Germany, and works on ZooMS and palaeoproteomics of Pleistocene bone assemblages. I.v.R. is currently a PhD student at Naturalis Biodiversity Centre, the Netherlands. M.S is assistant Professor in Palaeolithic Archaeology at Leiden University, the Netherlands, where M.R. is a researcher in Palaeolithic Archaeology. M.J.C. is Professor of Biomolecular Archaeology at the University of York, U.K. J.-J.H. is Professor at the MPI-EVA, Leipzig, and head of the Department of Human Evolution.

ORCID

Frido Welker http://orcid.org/0000-0002-4846-6104
Marie A. Soressi http://orcid.org/0000-0003-1733-7745
Isolde van Riemsdijk http://orcid.org/0000-0001-9739-6512
Jean-Jacques Hublin http://orcid.org/0000-0001-6283-8114
Matthew J. Collins http://orcid.org/0000-0003-4226-5501

Supplemental Data

Supplemental data for this article can be accessed at 10.1080/20548923.2016.1258825.

References

Allentoft, M.E., Collins, M.J., Harker, D., Haile, J., Oskam, C.L., Hale, M.L., Campos, P.F., Samaniego, J.A., Gilber, M.T.P., Willerslev, E., Zhang, G., Scofield, P., Holdaway, R.N. & Bunce, M. 2012. The Half-Life of DNA in Bone: Measuring Decay Kinetics in 158 Dated Fossils. *Proceedings of the Royal Society B*, 279(1748): 4724–33.

Behrensmeyer, A.K. 1978. Taphonomic and Ecologic Information from Bone Weathering. *Paleobiology*, 4(2): 150–62.

Benazzi, S., Peresani, M., Talamo, S., Fu, Q., Mannino, M.A., Richards, M.P. & J.-J. Hublin. 2014. A Reassessment of the Presumed Neandertal Remains from San Bernardino Cave, Italy. *Journal of Human Evolution*, 66: 89–94.

Blumenschine, R.J., Marean, C.W. & Capaldo, S.D. 1996. Blind Tests of Inter-Analyst Correspondence and Accuracy in the Identification of Cut Marks, Percussion Marks, and Carnivore Tooth Marks on Bone Surfaces. *Journal of Archaeological Science*, 23(4): 493–507.

Bocherens, H., Drucker, D.G., Billiou, D., Geneste, J.-M., & Kervazo, B. 2008. Grotte Chauvet (Ardèche, France): A "Natural Experiment" for Bone Diagenesis in Karstic Context. *Palaeogeography, Palaeoclimatology, Palaeoecology*, 266(3–4): 220–26.

Brown, S., Higham, T., Slon, V., Pääbo, S., Meyer, M., Douka, K., Brock, F., et al. 2016. Identification of a New Hominin Bone from Denisova Cave, Siberia Using Collagen Fingerprinting and Mitochondrial DNA Analysis. *Scientific Reports*, 6: 23559.

Buckley, M., Collins, M.J., Thomas-Oates, J. & Wilson, J.C. 2009. Species Identification by Analysis of Bone Collagen Using Matrix-Assisted Laser Desorption/ionisation Time-of-Flight Mass Spectrometry. *Rapid Communications in Mass Spectrometry*, 23(23): 3843–54.

Caron, F., d'Errico, F., Del Moral, P., Santos, F. & Zilhão, J. 2011. The Reality of Neandertal Symbolic Behavior at the Grotte Du Renne, Arcy-Sur-Cure, France. *PloS One*, 6(6): e21545.

Catak, S., Monard, G., Aviyente, V. & Ruiz-López, M.F. 2009. Deamidation of Asparagine Residues: Direct Hydrolysis versus Succinimide-Mediated Deamidation Mechanisms. *Journal of Physical Chemistry A*, 113(6): 1111–20.

Charlton, S., Alexander, M., Collins, M., Milner, N., Mellars, P., O'Connell, T.C., Stevens, R.E. & Craig, O.E. 2016. Finding Britain's Last Hunter-Gatherers: A New Biomolecular Approach to 'Unidentifiable' Bone Fragments Utilizing Bone Collagen. *Journal of Archaeological Science*, 73: 55–61.

Conard, N.J., Grootes, P.M. & Smith, F.H.. 2004. Unexpectedly Recent Dates for Human Remains from Vogelherd. *Nature*, 430(6996): 198–201.

Discamps, E., Delagnes, E., Lenoir, M. & Tournepiche, J.F. 2012. Human and Hyena Co-Occurrences in Pleistocene Sites: Insights from Spatial, Faunal and Lithic Analyses at Camiac and La Chauverie (SW France). *Journal of Taphonomy*, 10(3): 291–316.

van Doorn, N.L., Hollund, H. & Collins, M.J. 2011. A Novel and Non-Destructive Approach for ZooMS Analysis: Ammonium Bicarbonate Buffer Extraction. *Archaeological and Anthropological Sciences*, 3(3): 281–89.

van Doorn, N.L., Wilson, J., Hollund, H., Soressi, M. & Collins, M.J. 2012. Site-Specific Deamidation of Glutamine: A New Marker of Bone Collagen Deterioration. *Rapid Communications in Mass Spectrometry*, 26(19): 2319–27.

Enloe, J.G. 2012. Middle Palaeolithic Cave Taphonomy: Discerning Humans from Hyenas at Arcy-Sur-Cure, France. *International Journal of Osteoarchaeology*, 22(5): 591–602.

Evans, S., Briz i Godino, I., Álvarez, M., Rowsell, K., Collier, P., de Goodall, R.N.P., Mulville, J., Lacrouts, A., Collins, M.J. & Speller, C. 2016. Using Combined Biomolecular Methods to Explore Whale Exploitation and Social Aggregation in Hunter–gatherer–fisher Society in Tierra Del Fuego. *Journal of Archaeological Science: Reports*, 6: 757–67.

Fiddyment, S., Holsinger, B., Ruzzier, C., Devine, A., Binois, A., Albarella, U., Fischer, R., et al. 2015. Animal Origin of 13th-Century Uterine Vellum Revealed Using Noninvasive Peptide Fingerprinting. *Proceedings of the National Academy of Sciences*, 112(49): 15066–71.

Granger, J.-M. & Lévêque, F. 1997. Parure Castelperronienne et Aurignacienne: étude de Trois Séries Inédites de Dents Percées et Comparaisons. *Comptes Rendus de l'Académie Des Sciences - Series IIA - Earth and Planetary Science*, 325(7): 537–43.

Hao, P., Ren, Y., Alpert, A.J. & Sze, S.K. 2011. Detection, Evaluation and Minimization of Nonenzymatic Deamidation in Proteomic Sample Preparation. *Molecular & Cellular Proteomics*, 10(10): O111.009381.

Harvey, V.L., Egerton, V.M. Chamberlain, A.T., Manning, P.L. & Buckley, M. 2016. Collagen Fingerprinting: A New Screening Technique for Radiocarbon Dating Ancient Bone. *PloS One*, 11(3): e0150650.

Higham, T., Jacobi, R., Julien, M., David, F., Basell, L., Wood, R., Davies, W. & Ramsey, C.B. 2010. Chronology of the Grotte Du Renne (France) and Implications for the Context of Ornaments and Human Remains within the Châtelperronian. *Proceedings of the National Academy of Sciences*, 107(47): 20234–39.

Hoffmann, A., Hublin, J.-J., Hüls, M. & Terberger, M. 2011. The Homo Aurignaciensis Hauseri from Combe-Capelle–a Mesolithic Burial. *Journal of Human Evolution*, 61(2): 211–14.

von Holstein, I.C.C., Ashby, S.P., van Doorn, N.L., Sachs, S.M., Buckley, M., Meiri, M., Barnes, I., Brundle, A. & Collins M.J. 2014. Searching for Scandinavians in Pre-Viking Scotland: Molecular Fingerprinting of Early Medieval Combs. *Journal of Archaeological Science*, 41: 1–6.

Hublin, J.-J., Spoor, F., Braun, M., Zonneveld, F. & Condemi, S. 1996. A Late Neanderthal Associated with Upper Palaeolithic Artefacts. *Nature*, 381 (6579): 224–26.

Hublin, J.-J., Talamo, S., Julien, M., David, F., Connet, N., Bodu, P., Vandermeersch, B. & Richards, M.P. 2012. Radiocarbon Dates from the Grotte Du Renne and Saint-Césaire Support a Neandertal Origin for the Châtelperronian. *Proceedings of the National Academy of Sciences*, 109(46): 18743–48.

Ives, J.W., Froese, D.J., Collins, M.J. & Brock, F. 2014. Radiocarbon and Protein Analyses Indicate an Early Holocene Age for the Osseous Rod from Grenfell, Saskatchewan, Canada. *American Antiquity*, 79(4): 782–93.

Kuhn, B.F., Berger, L.R. & Skinner, J.D. 2010. Examining Criteria for Identifying and Differentiating Fossil Faunal Assemblages Accumulated by Hyenas and Hominins Using Extant Hyenid Accumulations. *International Journal of Osteoarchaeology*, 20(1): 15–35.

Lavaud-Girard, F. 1980. *Les faunes paléolithiques du Würm II et III dans le Sud-Ouest et le Centre-Ouest de la France*. Thèse de Spécialité, Université de Poitiers.

Lavaud-Girard, F. 1986. Les Gisements Castelperoniens de Quincay et de Saint-Césaire: Quelques Comparaisons Préliminaires-Les Faunes,. In *Préhistoire de Poitou-Charentes Problèmes Actuels*., ed. CTHS, 115–123. Poitiers.

Lévêque, F., Gouraud, G. & Bouin, F. 1997. Contribution à L'étude Des Occupations Préhistoriques de La Grotte de La Grande Roche de La Plématrie à Quincay (Vienne). *GVEP. Groupe Vendéen D'études Préhistoriques*, 33: 5–8.

Lévêque, F. & Miskovsky, J.-C. 1983. Le Castelperronien Dans Son Environnement Géologique. Essai de Synthèse à Partir de L'étude Lithostratigraphique Du Remplissage de La Grotte de La Grande Roche de La Plématrie (Quincay, Vienne) et D'autres Dépôts Actuellement Mis Au Jour. *L'Anthropologie*, 87(3): 369–91.

Lyman, R.L. 1994. *Vertebrate Taphonomy*. Cambridge University Press.

Lyndahl, T. & Nyberg, B. 1974. Heat-Induced Deamination of Cytosine Residues in Deoxyribonucleic Acid. *Biochemistry* 13, no. 16: 3405–3410.

Meiri, M., Lister, A.M., Collins, M.J., Tuross, N., Goebel, T., Blockley, S., Zazula, G.D., et al. 2014. Faunal Record Identifies Bering Isthmus Conditions as Constraint to End-Pleistocene Migration to the New World. *Proceedings of the Royal Society B*, 281(1776): 20132167.

Mikšík, I., Sedláková, P., Pataridis, S., Bortolotti, F., Gottardo, R. & Tagliaro, F. 2014. Prince Cangrande's Collagen: Study of Protein Modification on the Mummy of the Lord of Verona, Italy (1291–1329 Ad). *Chromatographia*, 77(21–22): 1503–1510.

Orlando, L., Ginolhac, A., Zhang, G., Froese, D., Albrechtsen, A., Stiller, M., Schubert, M., et al. 2013. Recalibrating Equus Evolution Using the Genome Sequence of an Early Middle Pleistocene Horse. *Nature*, 499(7456): 74–78.

Ren, D., Pipes, G.D., Liu, D., Shih, L.-Y., Nichols, A.C., Treuheit, M.J., Brems, D.N. & Bondarenko, P.V. 2009. An Improved Trypsin Digestion Method Minimizes Digestion-Induced Modifications on Proteins. *Analytical Biochemistry*, 392(1): 12–21.

Rendu, W., Beauval, C., Crevecoeur, I., Bayle, P., Balzeau, A., Bismuth, T., Bourguignon, L., et al. 2014. Evidence Supporting an Intentional Neandertal Burial at La Chapelle-Aux-Saints. *Proceedings of the National Academy of Sciences*, 111(1): 81–86.

Robinson, N.E. & Robinson, A.B. 2001. Prediction of Protein Deamidation Rates from Primary and Three-Dimensional Structure. *Proceedings of the National Academy of Sciences*, 98(8): 4367–72.

Robinson, N.E., Robinson, Z.W., Robinson, B.R., Robinson, A.L., Robinson, J.A., Robinson, M.L. & Robinson, A.B. 2004. Structure-Dependent Nonenzymatic Deamidation of Glutaminyl and Asparaginyl Pentapeptides. *The Journal of Peptide Research*, 63(5): 426–36.

Roussel, M. 2013. Méthodes et Rythmes Du Débitage Laminaire Au Châtelperronien: Comparaison Avec Le Protoaurignacien. *Comptes Rendus. Palevol*, 12(4): 233–241.

Roussel, M. & Soressi, M.. 2010. La Grande Roche de La Plématrie à Quinçay (Vienne). L'évolution Du Châtelperronien Revisitée. *Préhistoire Entre Vienne et Charente-Hommes et Sociétés Du Paléolithique*: 203–219.

Roussel, M. & Soressi, M. & Hublin, J.-J. 2016. The Châtelperronian Conundrum: Blade and Bladelet Lithic Technologies from Quinçay, France. *Journal of Human Evolution*, 95: 13–32.

Salesse, K., Dufour, E., Lebon, M., Wurster, C., Castex, D., Bruzek, J. & Zazzo, A. 2014. Variability of Bone Preservation in a Confined Environment: The Case of the Catacomb of Sts Peter and Marcellinus (Rome, Italy). *Palaeogeography, Palaeoclimatology, Palaeoecology*, 416: 43–54.

Schroeter, E.R. & Cleland, T.P. 2016. Glutamine Deamidation: An Indicator of Antiquity, or Preservational Quality? *Rapid Communications in Mass Spectrometry*, 30(2): 251–55.

Scotchler, J.W. & Robinson, A.B. 1974. Deamidation of Glutaminyl Residues: Dependence on pH, Temperature, and Ionic Strength. *Analytical Biochemistry*, 59(1): 319–22.

Simpson, J.P., Penkman, K.E.H., Demarchi, B., Koon, H., Collins, M.J., Thomas-Oates, J., Shapiro, B., Stark, M. & Wilson, J. 2016. The Effects of Demineralisation and Sampling Point Variability on the Measurement of Glutamine Deamidation in Type I Collagen Extracted from Bone. *Journal of Archaeological Science*, 69: 29–38.

Soressi, M. & Roussel, M. 2014. European Middle to Upper Paleolithic Transitional Industries: Châtelperronian. In *Encyclopedia of Global Archaeology*, 2679–2693. Springer New York.

Stiner, M.C., Kuhn, S.L., Surovell, T.A., Goldberg, P., Meignen, L., Weiner, S. & Bar-Yosef, O. 2001. Bone Preservation in Hayonim Cave (Israel): A Macroscopic and Mineralogical Study. *Journal of Archaeological Science*, 28(6): 643–59.

Talamo, S., Soressi, M., Roussel, M., Richards, M. & Hublin, J.-J. 2012. A Radiocarbon Chronology for the Complete Middle to Upper Palaeolithic Transitional Sequence of Les Cottés (France). *Journal of Archaeological Science*, 39, no. 1: 175–83.

Terberger, T., Street, M. & Bräuer, G. 2001. Der Menschliche Schädelrest Aus Der Elbe Bei Hahnöfersand Und Seine Bedeutung Für Die Steinzeit Norddeutschlands. *Archäologisches Korrespondenzblatt*, 31(4): 521–26.

Vaiglova, P., Bogaard, A., Collins, M.J., Cavanagh, W., Mee, C., Renard, J., Lamb, A., Gardeisen, A. & Fraser, R. 2014. An Integrated Stable

Isotope Study of Plants and Animals from Kouphovouno, Southern Greece: A New Look at Neolithic Farming. *Journal of Archaeological Science*, 42: 201–15.

Welker, F., Collins, M.J., Thomas, J.A., Wadsley, M., Brace, S., Cappellini, E., Turvey, S.T., et al. 2015a. Ancient Proteins Resolve the Evolutionary History of Darwin's South American Ungulates. *Nature*, 522(7554): 81–84.

Welker, F., Soressi, M., Rendu, W., Hublin, J.-J. & Collins, M.J. 2015b. Using ZooMS to Identify Fragmentary Bone from the Late Middle/Early Upper Palaeolithic Sequence of Les Cottés, France. *Journal of Archaeological Science*, 54: 279–86.

Welker, F., Hajdinjak, M., Talamo, S., Jaouen, K., Dannemann, M., David, F., Julien, M., Meyer, M., Kelso, J., Barnes, I., Brace, S., Kamminga, P., Fisher, R., Kessler, B., Stewart, J.R., Pääbo, S., Collins, M.J. & Hublin, J.-J. 2016. Palaeoproteomic evidence identifies archaic hominins associated with the Châtelperronian at the Grotte du Renne. *Proceedings of the National Academy of Sciences*, 113(40): 11162–67.

Wilson, J., van Doorn, N.L. & Collins, M.J. 2012. Assessing the Extent of Bone Degradation Using Glutamine Deamidation in Collagen. *Analytical Chemistry*, 84(21): 9041–48.